NON-INTRUSIVE SPIV OF FLOW BEHAVIOR INSIDE A 5X5 ROD BUNDLE WITH SPACER GRIDS

An Undergraduate Research Scholars Thesis

by

MATEUSZ MARCINIAK

Submitted to the Undergraduate Research Scholars program at
Texas A&M University
in partial fulfillment of the requirements for the designation as an

UNDERGRADUATE RESEARCH SCHOLAR

Approved by Research Advisors: Dr. Rodolfo Vaghetto
Dr. Thien Nguyen

May 2017

Major: Nuclear Engineering

ABSTRACT

Non-Intrusive SPIV of Flow Behavior Inside a 5x5 Rod Bundle with Spacer Grids

Mateusz Marciniak
Department of Nuclear Engineering
Texas A&M University

Research Advisor: Dr. Thien Nguyen
Research Advisor: Dr. Rodolfo Vaghetto
Department of Nuclear Engineering
Texas A&M University

New and improved thermal hydraulic data is essential for ensuring safe operation for Pressurized Water Reactors (PWR). Excessive fission product buildup on fuel rods produces uneven subcooling during operation which poses safety risks. Local sub-channel and fuel rod conditions are key parameters of interest in order to establish accurate critical heat flux parameters. Computational Fluid Dynamics (CFD) calculations are needed to produce these parameters but are very challenging due to the complex nature of two-phase and flow field in a PWR. CFD calculations rely on development of improved complex flow simulations with reasonably detailed flow structures with dynamic interaction of the flow. Having a better understanding of flow behavior in these geometries directly translates to the safety of nuclear power plants. To validate and benchmark contemporary CFD calculations, a scale modeled test facility was built. Experimental measurements were taken inside a 5x5 rod bundle with spacer grids to help validate current CFD codes. A non-intrusive approach was taken using Stereoscopic PIV (SPIV) techniques along with a Matching Index of Refraction (MIR) optical approach. This paper presents SPIV and pressure analyses on an existing Westinghouse 5x5 Spacer Grid facility.

DEDICATION

To my friends, and loved ones for helping me get to where I am today. To my teachers thank you for your patience and opening the doors for my education and research. I wouldn’t be the same person without all your help. Thank you all.

ACKNOWLEDGMENTS

None of this would be possible without the help of my colleagues and mentors at the Thermal Hydraulics lab. My mentors Dr. Thien Nguyen, Dr. Rodolfo Vaghetto, Dr. Saya Lee, and Dr. Yassin Hassan. All your endless help and wisdom made this possible. Special thanks to upcoming Dr. Nolan Goth, Dr. Mason Childs, Dr. Nico Quintanar, M.S. Philip Jones. You guys showed me the ropes and inspire me every day to be a better and smarter me. To all my fellow undergraduates friends/colleagues whom I shared laughs and frustration and everything in between.

CONTRIBUTORS AND FUNDING SOURCES

Contributors

This work was supported by a thesis committee consisting of Professor Rodolfo Vaghetto [advisor], Professor Thien Nguyen [advisor] of the Department of Nuclear Engineering and Mason Childs M.S. of the Department of Nuclear Engineering. The data analyzed for Chapter 4 was provided by Professor Thien Nguyen.

NOMENCLATURE

PWR	Pressurized Water Reactor
CFD	Computational Fluid Dynamics
PIV	Particle Image Velocimetry
SPIV	Stereoscopic Particle Image Velocimetry
MIR	Matched Index of Refraction
FFT	Fast Fourier Transform
FEP	Fluorinated Ethylene-Propylene Plastic
TR-SPIV	Time Resolved Stereoscopic PIV

TABLE OF CONTENTS

Page

LIST OF FIGURES

FIGURE Page

1. INTRODUCTION

1.1 5x5 Rod Bundle

A scale-downed geometry of a full fuel assembly was modeled using a 5x5 rod bundle. Major features to be investigated in the test bundle include cross-flow mixing between sub-channels, anisotropic turbulent diffusion, and secondary flows. These phenomena can occur near the spacer grid due to the edge shape patterns in the grid and angle of the mixing vane blades. Turbulence decreases as the flow becomes more developed further away from the spacer grid. There are two noteworthy cross-flow mixing in rod bundle geometry: macroscopic mixing, due to the time mean lateral or azimuthal velocity, and microscopic turbulent mixing caused by fluctuating velocity [1]. Understanding the mixing mechanism can shed more light on the micro and macroscopic mixing taking place in current pressurized water reactor (PWR)s. Additionally we seek to solve flow around cylindrical rods. It is a common occurrence especially in nuclear plant systems involving boundary layers, separation, and vortice dynamics.

Described flow fields are especially challenging since they involve a large number of complex configurations. These flow structures in fuel rod bundles of Light Water Reactors reflect heat removal from the surface of the fuel. Spacer grids support the fuel bundle geometry and produce an effective mixing effect through attachment of flow deflectors that stimulate heat transfer. Current computational fluid dynamics (CFD) codes aim to predicting the complex flow behavior in the core particularly in the spacer grid. These models require further analysis and experimental treatment to be recognized as reliable. Improved velocity data would aid in reliable design and performance criteria for validation of these models. Spacer grids also allow for mixing of coolant flow in subchannels through attachment of various flow promoters at strap edges. Efforts are underway to develop optimized spacer grids that can effectively mix coolant flow in the sub channel geometry.

1.2 Matched Index of Refraction

Flow studies involving complex geometries are made simpler using a matched index of refraction (MIR) [2]. The approach involves the phenomena of light passing through a material with a similar index of refraction. Normally when light passes through a material it gets bent at the interface of the materials which creates a distorted image or hidden areas within that same image. However by utilizing MIR we are able to limit and eliminate this distortion by matching the index of refraction between the materials creating a clear image such as when we look through glass. This approach allows for an area of interest to be captured and measured. The MIR technique has become more widespread with the introduction of PIV technique and developments of new and advanced materials. The technique itself is not complicated however concerns like price, viscosity, and flammability of the working fluid complicate the technique.

Utilizing a MIR approach with PIV technique to render full field velocity distribution at various scales of a rod bundle. The spacer grid introduced an attenuation of the vorticity magnitude however a counteracting phenomenon suppressed the attenuation. Averaged data showed a rather uniform direction velocity profile after the spacer grid while the downstream illustrated a no slip wall profile. A large-scale undeveloped turbulent flow was also seen around the spacer grid due a separation above the spacer grid. The phenomena appears in the inlet of the spacer while braking up the developed main flow in the sub-channel [3].

1.3 Turbulent Flow Structures in a Rod Bundle Assembly

Common mixing vanes used in rod bundle experiments were split type and swirl type. A split type enhances the flow mixing between the sub-channels through the gaps. A swirl type is known to create a strong vortex which disperses thermal energy within a sub-channel instead of mixing between the sub-channels.[4]The swirl types also has larger primary vane along with secondary vanes in a sub-channel. Chang's experiment showed that the split type had a couple of symmetric vortices generated by the split vanes within a sub-channel at the inner and middle sub-channel. Size of vortex was noted to be one fourth of the rod pitch. Small localized vortices contributed thermal mixing in a very narrow region within the sub-channel. Cross flow at the four gaps in a sub-channel is very vigorous and provides good energy exchange between the nearby sub-channels. The swirl type created one large vortex elliptical in shape generated within a sub-channel at the inner and middle sub-channels. The size of vortex was about 2.6 times larger than the split type vane. The swirling flow was shown to flatten the temperature profile caused by the heat flux from the fuel rod surface. Cross flow was also effective for the mixing of sub-channels but inter channel mixing was less than the split type.

1.4 CFD validation for PWR fuel assemblies

Flow field investigation of the flow field is done by use of mixing vanes to develop and measure lateral flow field at various elevations of the grid. A technique of choice to visualize flow field is PIV utilizing MIR approach.[5] To truly measure with confidence between PWR operating conditions high Reynolds numbers would also need to be investigated along with future heated rod assemblies. Test data conducted showed that just downstream of the mixing vane lateral flow field is dominated by mixing vane geometry. Further downstream approaching the next spacer grid vane patterns and lateral boundary conditions play a more evident effect on flow within the sub-channels. The modeled 5x5 rod bundle is designed to be representative of a 17x17 fuel bundle design. Rod pitch, rod diameter, and mixing vane features are representative of the full scale design. In a comparison of lateral flow field velocity CFD calculations and PIV data showed differences in vector density, higher in the CFD model. The same lateral flow structure was seen in both methods showing two vortices in the sub-channel center with the same swirl flow and axial development in different axial elevations [6].

1.5 Stereoscopic Particle Image Velocimetry

Stereoscopic PIV utilizes two cameras to record a simultaneous images with an overlapping region of interest. This region is illuminated by the use of a laser and tracer particles. The use of two cameras allows for the extraction of the out of plane motion of the flow we are studying. All stereoscopic systems must satisfy certain basic requirements of recording two simultaneous but different views of the same object plane. The two views are then combined using an in house code or other algorithms to reconstruct the three-dimensional flow field [7].

Velocity calculations were done utilizing the same approach as [3] given by

$$\overline{A} = \frac{\sum_{i=1}^{N} A_i \overline{X}}{N} \tag{1.1}$$

Vorticity calculations are done using

$$\vec{\omega} = \nabla \times \vec{v} = (\frac{\partial v_z}{\partial y} - \frac{\partial v_y}{\partial z}), (\frac{\partial v_x}{\partial z} - \frac{\partial v_z}{\partial x}), (\frac{\partial v_y}{\partial x} - \frac{\partial v_x}{\partial y}) \tag{1.2}$$

2. EXPERIMENTAL SET-UP

2.1 Facility

The experiments were conducted at the Thermal Hydraulic laboratory at Texas A&M University (TAMU). The flow loop contains a variable speed pump, 1135.62 liter storage tank, ultrasonic flowmeter, flow straightener (honeycomb) mesh, and MIR test section. Water was used as the working fluid flowing from bottom of the test section upwards, to model real PWR core flow. Flow rate was controlled using a frequency controlled (VFD) and a control valve in the main loop to allow for repeatability of flow rates. The pump and loop have been sized up to achieve a higher Reynolds Number (Re = 28,000) however test loop can achieve a much higher Reynolds Numbers. The test bundle is a 5x5 rod bundle that has been scale to be representative of a 17x17 fuel bundle. The rod bundle pitch (12.6 mm), rod diameter (9.5 mm) and grid features include rod support and mixing vane consist with the 17x17 bundle. There are 25 rods in the test bundle with no thimble tube locations in the rod bundle. The bundle also includes multiple grids spaced on a typical axial grid of 510 mm. the spacer grids have mixing vanes on them. Some spacer grids locations contain no vaned support grids but are away from measurement regions.

Two digital CMOS Phantom M310 cameras for capturing PIV measurements. The high speed Phantom M310 camera have a full resolution of1280x800 pixel display with pixel size of 20x20μm^2 and 12 bit depth and store images to their internal 12GB high speed RAM. Silver coated hollow glass micro particles of mean diameter and density of 16 μm and 1.6 $g\,cm^{-3}$, respectively.

2.2 Test Rods

The test rods used in the bundle were fabricated using a fluorinated ethylene-propylene plastic (FEP) with dimensions of 9.5 OD x 9 ID x 1270 mm long with a +- 0.0762 mm tolerance in all dimensions. FEP tubes were chosen to match the refractive index of water to allow for an optically clear test area when immersed with water. Thick plastic tubes of acrylic and polycarbonate were inserted at the top and bottom to maintain rod rigidity during testing and measurements. Rods are also maintained at the appropriate rod pitch in the ungridded regions and maintain integrity under flowing conditions. Flow housing is square in shape with a small gap between the grids and housing inner walls. The walls are made of transparent acrylic to provide optical transparency for the laser and cameras system. Pressure taps are located on the housing walls so pressure drop measurements are at different regions of the test bundle. It is also essential to have pressure reading near the SPIV measurement area. Flow entering from the bottom is conditioned through a flow straightener to ensure pure vertical flow. The vertical flow from the pump is passed through a plenum region where flow maintains its axial direction while reducing in cross section area as flow travels through it.

2.3 SPIV

SPIV uses two cameras to record simultaneous but distinct views of the same region of interest illuminated by a laser plane. the illuminated plane contains a flow that has been seeded with appropriate tracer particles. There is also information contained in the two camera views to extract the out of plane motion of tracer particles. The technique is employed since a single view cannot resolve the out of plane dimension of the flow field. By the addition of a second different view of the second camera two additional equations may be used to solve for the three-dimensional information. our eyes record two off axis view simultaneously and our brain is then able to combine the two views together in real time to provide the desired three-dimensional view of the flow field. Common with this technique we employ a Scheimpflug lens to allow for us to correct one dimension of our measurement plane to help minimize errors of the the technique. All stereoscopic systems

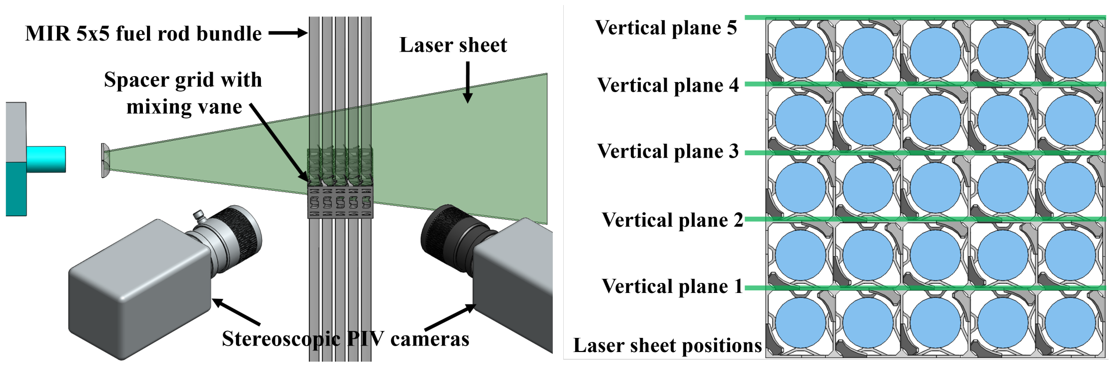

Figure 2.1: Experimental setup of Time-resolved stereoscopic PIV measurements in the fuel bundle with the spacer grid (left), and SPIV laser sheet positions (right).

must satisfy recording two simultaneous with different views of the same intended object. These two camera views are combined using different algorithms to reconstruct the three dimensional velocity profile.Figure 2.1 shows the PIV experimental setup that consists of a two-dimensonal three-component (2D3C) time resolved stereoscopic PIV (TR-SPIV) system.

All PIV images captured by two Phantom cameras were processed by advanced multi-pass, multi-grid processing algorithms. These are based on robust phase correlation (RPC) algorithms that have been implemented in the PRANA codes by Virginia Tech [8], [9]. Three iterations were performed and the final passes had a 75% window overlap necessary for correct SPIV calculations. Inside each pass, statistical validations were performed to identify and replace erroneous vectors as part of post-processing and validation of acquired data. A median filter is applied and standard deviations of the neighboring vectors were used to filter out spurious vectors. Lastly SPIV processing, pairs of two-dimensional displacement fields calculated from cameras were reconstructed using mapping functions to obtain three-component velocity fields to match the test facility geometry. These vectors should be able to fully reconstruct the measured test section to ensure proper optical measurements. All Post processing was done by Dr. Thien Nguyen.

3. RESULTS AND DATA ANALYSIS

The flow through the visualization section was observed for vertical plane 1 as shown in Figure 2.1 . The size of the region observed by the PIV cameras was approximately 50 millimeter along the x axis and 33 mms along the y axis. The viewing window was oriented 21 millimeters axially above the spacer grid with mixing vane as seen in Figure 3.1. This position of the viewing window was selected for its matching index of refraction (MIR) properties, which began downstream of the spacer grid and was as close as manageable with the current experimental setup.

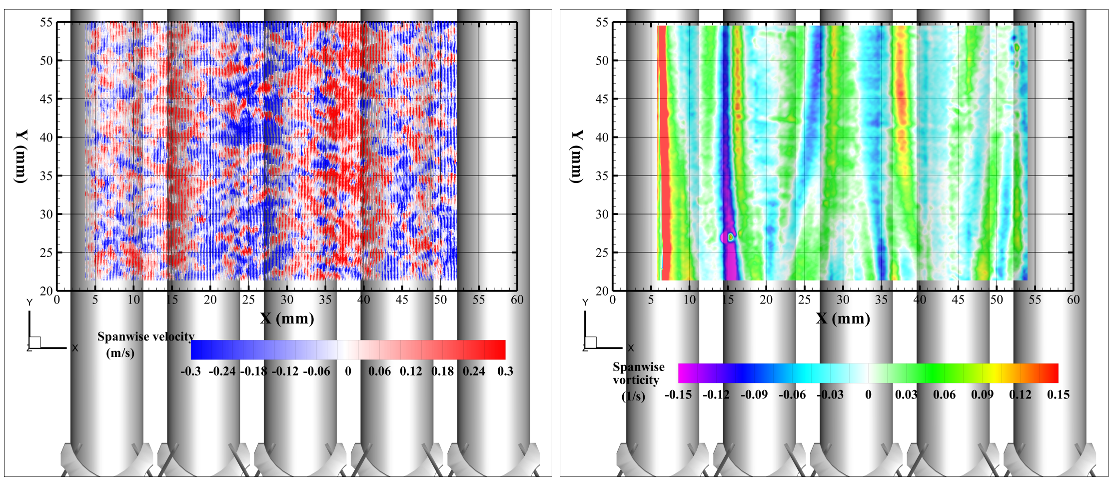

Figure 3.1: Instantaneous (left) and mean velocity (right) fields obtained from TR-SPIV measurements in the vertical plane 1. Color contour shows the magnitude of the spanwise velocity, W.

Figure 3.1 shows the results for single velocity measurements and mean velocity calculated from multiple PIV runs at a Re condition of 14000. The spanwise component of the velocity vector, W is indicated by the color contour. The instantaneous velocity profile shows a seemingly random distribution of velocity components which satisfy a fully developed turbulent flow regime. In the mean velocity profile, the flow direction is dominated by the axial component of the velocity, V, especially in the area further from the mixing vane. These results show good agreement with previous 2D measurements of velocity profiles above the mixing vane [10].

.

4. SUMMARY, CONCLUSIONS, AND FUTURE WORK

4.1 Future Study

More measurements are currently being done on the facility involving changing the spacer grid locations Same measurements will be done to cross validate our own data along with CFD models. With more data we can expect to get a better validation and understanding of mixing vane behavior. In addition another facility is in process of being built that will tackle heated flow in the future as means of more thorough modeling of Westinghouse PWRs reactor. Upon completion similar measurements will be done and validated against CFD calculations and these current results.

4.2 Challenges

FEP tubes do not achieve a fully MIR therefore there is difficulty is acquiring the best optical measurements. In numerous cases achieving the best results required hours of constant adjustments in order to achieve good results. More computational time is spent in post processing to eliminate erroneous results due to optical clarity of the facility.

The experimental facility is made up of numerous different materials through which the camera has to look through which induces more error and camera adjustment to account for all the refraction going on in each material. Accurate thickness measurements had to be taken for each material to account for total refraction in the facility. We assume that the material thickness is constant throughout however the accuracy is based on the material fabrication process. This indirectly introduces an error in flow visualization. In the post processing phase, measurements are used for reconstruction of the test facility. If the results produce an accurate reconstruction of the fuel bundle and spacer grid then the data acquired has more validation and accurately accounted for the material composition inside.

Dirt particles inside the facility also provided issues in available measurement areas.

Certain segments of the test facility contain dirt particles from when the facility was first fabricated. FEP tubes were put together through attaching an acrylic rod at the top and bottom of the FEP tube. The tube acts as a sleeve and is fully supported by the acrylic rods at the top and bottom. During the original fabrication dirt was trapped inside and provides a vacancy when taking measurement. Any data acquired around the dirt particle cannot be considered because it is opaque. Additionally certain areas of the test section introduce air bubbles that are trapped inside. When shinning a laser through an air bubble the scattering encountered blurs area of the image. These areas do not provide enough information to visualize the flow creating "dead spots" in the image. Measurementation had to be elevated to a different point axially on the facility to avoid any air bubbles that formed.

SPIV measurements were taken at a set Reynolds Number. When attempting to raise the Reynolds number for measurementation at a higher regime the facility began to vibrate slightly. however when measurement were taken the results were too skewed to produce an accurate velocity field. It would take too much post processing work to validate and clean up the results. As a means of validation we were confined to comparing results with only the 14,000 Reynolds flow regime. By producing more results around different Reynolds number it is easier to validate as other have performed similar measurements but at higher Reynolds numbers.

REFERENCES

[1] S. K. Yang and M. K. Chung, "Turbulent flow through spacer grids in rod bundles," *Journal of Fluids Engineering*, vol. 120, no. 4, pp. 786–791, 1998.

[2] N. Amini and Y. A. Hassan, "An investigation of matched index of refraction technique and its application in optical measurements of fluid flow," *Experiments in fluids*, vol. 53, no. 6, pp. 2011–2020, 2012.

[3] E. E. Dominguez-Ontiveros and Y. A. Hassan, "Non-intrusive experimental investigation of flow behavior inside a 5×5 rod bundle with spacer grids using piv and mir," *Nuclear Engineering and Design*, vol. 239, no. 5, pp. 888–898, 2009.

[4] S. K. Chang, S. K. Moon, W. P. Baek, and Y. D. Choi, "Phenomenological investigations on the turbulent flow structures in a rod bundle array with mixing devices," *Nuclear engineering and design*, vol. 238, no. 3, pp. 600–609, 2008.

[5] M. E. Conner, E. Baglietto, and A. M. Elmahdi, "Cfd methodology and validation for single-phase flow in pwr fuel assemblies," *Nuclear Engineering and Design*, vol. 240, no. 9, pp. 2088–2095, 2010.

[6] E. E. Dominguez-Ontiveros, Y. A. Hassan, M. E. Conner, and Z. Karoutas, "Experimental benchmark data for pwr rod bundle with spacer-grids," *Nuclear Engineering and Design*, vol. 253, pp. 396–405, 2012.

[7] A. K. Prasad, "Stereoscopic particle image velocimetry," *Experiments in fluids*, vol. 29, no. 2, pp. 103–116, 2000.

[8] A. Eckstein and P. P. Vlachos, “Assessment of advanced windowing techniques for digital particle image velocimetry (dpiv),” *Measurement Science and Technology*, vol. 20, no. 7, p. 075402, 2009.

[9] A. Eckstein and P. P. Vlachos, “Digital particle image velocimetry (dpiv) robust phase correlation,” *Measurement Science and Technology*, vol. 20, no. 5, p. 055401, 2009.

[10] M. E. Conner, Y. A. Hassan, and E. E. Dominguez-Ontiveros, “Hydraulic benchmark data for pwr mixing vane grid,” *Nuclear Engineering and Design*, vol. 264, pp. 97–102, 2013.